

This discussion paper is/has been under review for the journal *Atmospheric Chemistry and Physics (ACP)*. Please refer to the corresponding final paper in *ACP* if available.

**Laboratory studies of
the atmospheric
aging of wood smoke**

A. P. Grieshop et al.

Laboratory investigation of photochemical oxidation of organic aerosol from wood fires – Part 1: Measurement and simulation of organic aerosol evolution

A. P. Grieshop, J. M. Logue, N. M. Donahue, and A. L. Robinson

Center for Atmospheric Particle Studies, Carnegie Mellon University, Pittsburgh, PA, USA

Received: 3 July 2008 – Accepted: 7 July 2008 – Published: 18 August 2008

Correspondence to: A. L. Robinson (alr@andrew.cmu.edu)

Published by Copernicus Publications on behalf of the European Geosciences Union.

Title Page

Abstract

Introduction

Conclusions

References

Tables

Figures

◀

▶

◀

▶

Back

Close

Full Screen / Esc

Printer-friendly Version

Interactive Discussion

Abstract

Experiments were conducted to investigate the effects of photo-oxidation on organic aerosol (OA) in wood smoke by exposing diluted emissions from soft- and hard-wood fires to UV light in a smog chamber. Particle- and gas-phase concentrations were monitored with a suite of instruments including a Proton Transfer Reaction Mass Spectrometer (PTR-MS), an Aerosol Mass Spectrometer (AMS) and a thermodenuder to measure aerosol volatility. The measurements highlight how in-plume processing can lead to considerable evolution of the mass and volatility of biomass burning OA. Photochemical oxidation produced substantial new OA, increasing concentrations by a factor of 1.5 to 2.8 after several hours of exposure to typical summertime hydroxyl radical (OH) concentrations. Less than 20% of this new OA could be explained using the measured decay of traditional secondary organic aerosol (SOA) precursors and a state-of-the-art SOA model. Aging also created less volatile OA; at 50°C between 50 and 80% of the fresh primary OA evaporated but only 20 to 40% of aged OA. Therefore, the data provide additional evidence that primary OA is semivolatile. They also raise questions about the current approach used to simulate OA in chemical transport models, which assume that primary OA are non-volatile but that SOA is semivolatile. Predictions of a volatility basis-set model that explicitly tracks the partitioning and aging of low-volatile organics are compared to the chamber data. This model demonstrates that the OA production observed in these experiments can be explained by oxidation of low volatility organic vapors. The basis-set model can also simulate observed changes in OA volatility and composition, predicting the OA production and the increased oxygenation and decreased volatility of the OA.

1 Introduction

Combustion of biomass is a major source of gas- and particle-phase air pollutants on the urban (Robinson et al., 2006; Schauer and Cass, 2000), regional (Wotawa and

ACPD

8, 15699–15737, 2008

Laboratory studies of the atmospheric aging of wood smoke

A. P. Grieshop et al.

Title Page

Abstract

Introduction

Conclusions

References

Tables

Figures

◀

▶

◀

▶

Back

Close

Full Screen / Esc

Printer-friendly Version

Interactive Discussion



**Laboratory studies of
the atmospheric
aging of wood smoke**A. P. Grieshop et al.

[Title Page](#)[Abstract](#)[Introduction](#)[Conclusions](#)[References](#)[Tables](#)[Figures](#)[◀](#)[▶](#)[◀](#)[▶](#)[Back](#)[Close](#)[Full Screen / Esc](#)[Printer-friendly Version](#)[Interactive Discussion](#)

Trainer, 2000) and global (Lelieveld et al., 2001) scales. Biomass-burning is estimated to contribute approximately one-third of total $PM_{2.5}$ in the US (Watson, 2002) and 90% of the global emissions of primary particulate organic carbon (OC) from combustion sources (Bond et al., 2004). Light-absorbing carbonaceous aerosols emitted by large scale biomass fires in South America, Asia and Africa are thought to have continental- and global-scale climate impacts (Andreae et al., 2004; Ramanathan et al., 2007). Biomass burning encompasses a range of sources including space heating, cooking, wildfires and prescribed burns. The emissions from all of these sources are highly variable, with fuel type, moisture content and combustion conditions all having large influences on the chemical and physical make up of gas- and condensed-phase emissions (Reid et al., 2005).

Biomass burning emits a complex mixture of organics that span a wide range of volatility. Some of the organics have very low vapor pressures and thus partition directly into the particle phase creating primary organic aerosol (POA). Biomass burning also emits volatile organic compounds (VOCs); some of these, such as light aromatics, are known precursors for secondary organic aerosol (SOA). SOA is formed when photo-oxidation of VOCs produces low-volatility products that partition into the condensed phase. Source dilution experiments have shown that a large fraction of wood smoke POA is semivolatile (Lipsky and Robinson, 2006; Shrivastava et al., 2006). Therefore, a pool of low-volatility organic vapors exists in plumes.

A number of field studies report substantial production of organic aerosol (OA) in biomass burning plumes that cannot be explained with current models (Reid et al., 2005). Lee et al. (2008) inferred a 1.5- to 6-fold enhancement of OA in a prescribed burn plume within 3 to 4 h after emission. Sizeable production has also been reported for savannah fire plumes in South Africa (Abel et al., 2003; Hobbs et al., 2003). Concentrations of organic acids can also be enriched in biomass-burning plumes (Nopmongcol et al., 2007; Peltier et al., 2007; Reid et al., 1998). Nopmongcol et al. (2007) proposed that the excess OA levels were due to acid-catalyzed heterogeneous SOA formation; Lee et al. (2008) speculated that they might be due to enhanced isoprenoid

emissions.

Recent laboratory experiments have shown that photochemical aging of semi-volatile organic compounds (SVOCs) in diluted diesel exhaust produces large amounts of OA, much more than can be explained with traditional SOA precursors (Robinson, 2007; Sage et al., 2008; Weitkamp et al., 2007). That work demonstrated the important linkages between the gas-particle partitioning of SVOCs and aging; elucidating this relationship for other emission sources is an important need.

This paper describes laboratory aging experiments carried out to investigate OA production in emissions from hard- and soft-wood fires at plume-like conditions. The experiments are designed to bridge the gap between field observations and laboratory studies of source emissions and SOA formation from single precursors. The specific objectives include:

1. quantifying the production of OA due to photo-oxidation of biomass smoke plumes;
2. assessing whether or not this production can be described by measured decay of known SOA precursors;
3. measuring the effects of aging on OA volatility; and
4. comparing the measured behavior to predictions of the model proposed by Robinson et al. (2007) that explicitly accounts for partitioning and aging of primary emissions.

2 Methods

The effects of photochemical aging on wood smoke were investigated by injecting emissions into the Carnegie Mellon University (CMU) smog chamber and then aging the diluted emissions via photochemistry initiated by UV lights. The smog chamber is a temperature-controlled room containing a 12 m³ Teflon-bag (Presto et al., 2005a).

Laboratory studies of the atmospheric aging of wood smoke

A. P. Grieshop et al.

Title Page

Abstract

Introduction

Conclusions

References

Tables

Figures

◀

▶

◀

▶

Back

Close

Full Screen / Esc

Printer-friendly Version

Interactive Discussion



Before each experiment, the chamber was cleaned by irradiation, heat (40°C), and continuous flushing with dry, HEPA-filtered and activated-carbon-filtered air overnight. After cleaning, the lights were turned off, and the chamber temperature was reduced to 22°C with an initial relative humidity of ~5%.

5 A small amount of exhaust was added to the chamber through a heated inlet connected to a small wood stove (Cabela's Shepherd Packer Stove). The fuels included (in separate experiments) mixed hardwoods, Laurel Oak and Yellow Pine and injection occurred during a variety of combustion conditions, from smoldering to active flaming. The fuel wood was cut into small (approximately 4×4×20 cm) pieces and the fire was
10 allowed to burn for ~30 min to allow the stove and chimney to reach a normal operating temperature. Exhaust was injected into the chamber using ejector diluter (Dekati DI 1000) connected to the stack of the stove about 30 cm above the fire box. The ejector diluter was operated with HEPA and activated-carbon-filtered air heated to 350°C. All sampling and transfer lines were also maintained at 350°C. Upon entering the chamber,
15 the exhaust is rapidly diluted and cooled. Initial particulate matter concentrations were tens to hundreds of $\mu\text{g m}^{-3}$ of predominantly carbonaceous material. Conditions were thus "near ambient", consistent with plumes downwind of a point source. In two experiments, NO_x levels in the wood smoke were very low, so additional NO was injected with a target concentration of 50–150 ppb.

20 After allowing time for mixing and initial data collection, the UV lights in the smog chamber (General Electric Model 10526 blacklights) were turned on to initiate photo-oxidation reactions. These lights yield an NO_2 photolysis rate (J_{NO_2}) of approximately 0.2 min^{-1} (roughly equivalent to solar radiation at a 70° zenith angle; Carter et al., 2005). The experiments were conducted at $22 \pm 2^\circ\text{C}$. The basic experimental
25 procedures were similar to the diesel aging experiments described by Weitkamp, et al. (2007), with the addition of continuous aerosol black carbon (BC) and volatility measurements and a more extensive set of VOC measurements.

**Laboratory studies of
the atmospheric
aging of wood smoke**A. P. Grieshop et al.

[Title Page](#)[Abstract](#)[Introduction](#)[Conclusions](#)[References](#)[Tables](#)[Figures](#)[◀](#)[▶](#)[◀](#)[▶](#)[Back](#)[Close](#)[Full Screen / Esc](#)[Printer-friendly Version](#)[Interactive Discussion](#)

2.1 Instrumentation

The evolution of the physical and chemical properties of the aerosol was monitored with continuous and semi-continuous gas- and particle-phase instrumentation. Gas-phase measurements included: CO₂ (LI-820, Li-Cor Biosciences), CO (Model 300A, API-Teledyne), NO_x (Model 200A, API-Teledyne) and O₃ (Model 1008-PC, Dasibi). VOCs were measured with a Proton Transfer Reaction Mass Spectrometer (PTR-MS, Ionicon) and semi-continuous Gas Chromatograph-Mass Spectrometer (GC-MS, based on the design of Millet et al. (2005)). The PTR-MS and GC-MS systems were calibrated using standards (TO-15 Standard, Spectra Gases, a custom blend of light- and heavy hydrocarbons from Scott Gases, and vaporized toluene, acetone, acetonitrile and acetaldehyde). The PTR-MS was operated in full-scan mode (scanning from 22 to 142 amu) during the first experiment, after which masses showing substantial change during the course of the experiment were selected; the remaining experiments were run in selected-ion mode with a time resolution of ~2.5 min.

Aerosol size and composition distributions were measured with an Aerodyne Quadrupole Aerosol Mass Spectrometer (AMS; Canagaratna et al., 2007) and two Scanning Mobility Particle Sizers (SMPS, TSI, Inc., Models 3071 and 3080). The SMPS systems sampled particles with mobility diameters (D_{ma}) from 16 to 760 nm, overlapping with the AMS particle transmission window (Canagaratna et al., 2007). The AMS alternated every 10 s between mass spectrum (MS) scanning, Jump Mass Spectrum (JMS; Crosier et al., 2007) and particle time of flight (PToF) modes with a sample averaging time of 5 min and a vaporizer temperature of 600°C. The AMS signal at m/z 44 was corrected for the contribution from gas-phase CO₂ and the particle-phase contribution at m/z 28 (CO⁺ and potentially C₂H₄⁺) was estimated via comparison with particle-free samples¹. AMS data are here used to quantify organic aerosol

¹Grieshop, A. P., Donahue, N. M., and Robinson, A. L.: Laboratory investigation of photochemical oxidation of organic aerosol from wood fires – Part 2: Analysis of aerosol mass spectrometer data, TBD, in preparation, 2008.

Laboratory studies of the atmospheric aging of wood smoke

A. P. Grieshop et al.

Title Page

Abstract

Introduction

Conclusions

References

Tables

Figures

◀

▶

◀

▶

Back

Close

Full Screen / Esc

Printer-friendly Version

Interactive Discussion



concentration; detailed discussion of chemical composition measurements is contained in a companion paper¹.

Aerosol black carbon (BC) was measured with a Magee Scientific 7-channel aethalometer (Model AE-31). BC was quantified using either the 880 or 590 nm channel; these longer wavelengths are more strongly associated with BC versus other light-absorbing (brown) carbonaceous species (Kirchstetter et al., 2004). There was no evidence of secondary production of light-absorbing aerosols during aerosol aging at these wavelengths. Aethalometer attenuation measurements were corrected for particle loading effects using the method of Kirchstetter and Novakov (2007).

At the end of every experiment but one, filter packs containing two pre-fired quartz-fiber filters were collected and analyzed with a Sunset Laboratory TOT Organic Carbon/Elemental Carbon (OC/EC) Analyzer using a modified version of the NIOSH 5040 protocol (Subramanian et al., 2004). The back-up filter is used to correct the front filter for OC positive artifact from gas phase organics; see (Subramanian et al., 2004; Turpin et al., 2000). The filter results were compared to the aethalometer and AMS data. The aethalometer BC concentration and filter EC concentrations were in good agreement (slope=0.83, $R^2=0.99$); AMS organic and filter OC were well correlated ($R^2=0.97$).

Aerosol volatility was investigated using a thermodenuder (TD) system which heated a sample continuously drawn from the chamber and then stripped the evaporated vapors using an activated-carbon denuder (An et al., 2007). The residence time in the heated section was approximately 16 s. The TD was operated at gas temperatures between 50 and 85°C. An SMPS and the AMS were used to characterize the aerosol downstream of the TD and on a bypass line maintained at 25°C. The measurements alternated between these two lines every 15–30 min. Total number loss in the TD system was found to be less than 2% at ambient temperatures (An et al., 2007) and AMS mass loss in the system (in bypass mode) was less than 5%.

Laboratory studies of the atmospheric aging of wood smoke

A. P. Grieshop et al.

[Title Page](#)[Abstract](#)[Introduction](#)[Conclusions](#)[References](#)[Tables](#)[Figures](#)[◀](#)[▶](#)[◀](#)[▶](#)[Back](#)[Close](#)[Full Screen / Esc](#)[Printer-friendly Version](#)[Interactive Discussion](#)

2.2 Data analysis

2.2.1 Quantifying OA production

Quantifying the production of OA requires correcting for losses of particles and vapors to the chamber walls. These corrections have been extensively discussed in earlier papers (Grieshop et al., 2007; Weitkamp et al., 2007; Pierce et al., 2008). In this paper we use two independent methods to correct for wall losses. First, we use black carbon as a tracer for primary emissions. Under the assumption that the aerosol is internally mixed OA and BC have the same wall-loss rate and changes in the ratio of OA to BC mass indicate condensation or evaporation of semi-volatile vapors. We quantify these changes using the OA enhancement ratio (ER):

$$ER(t) = \frac{\frac{OA(t)}{BC(t)}}{\frac{OA(t=t_0)}{BC(t=t_0)}} \quad (1)$$

where t_0 refers to the time when the lights were turned on.

The second approach used to estimate OA production is based on calculating particle mass balance inside the chamber as discussed by Weitkamp et al. (2007). Briefly, the SMPS data are corrected for wall-loss using a first order wall-loss rate measured during periods with no production (when the black lights are off). Both approaches assume that the OA deposited to the walls remains in equilibrium with the suspended material. Evidence from other chamber aging and dilution experiments suggests that this is generally the case (Grieshop et al., 2007; Weitkamp et al., 2007) and that there are negligible direct losses of organic vapors to the wall².

OA production was also estimated by decomposing the AMS organic mass spectra (MS) into primary and secondary MS as outlined by Sage et al. (2008). This method and results from its application are discussed in a companion paper¹.

²Epstein, S. A. and Donahue, N. M.: Adsorptive wall losses of semi-volatile vapors in smog-chamber experiments, in preparation, 2008.

Title Page

Abstract

Introduction

Conclusions

References

Tables

Figures

◀

▶

◀

▶

Back

Close

Full Screen / Esc

Printer-friendly Version

Interactive Discussion



2.2.2 OA Volatility

The AMS measurements made with the TD system were analyzed to quantify the OA volatility throughout the experiment. Organic mass evaporation from the aerosol phase during residence in the TD is presented as the mass fraction remaining (MFR), defined as the ratio of the OA mass concentration measured through the TD (C_{TD}) to that measured through the bypass line (C_{bypass}):

$$\text{MFR} = \frac{C_{TD}}{C_{bypass}} \quad (2)$$

2.2.3 SOA Modeling

The measured decay of VOCs was used in conjunction with the SOA model SOAM II to estimate the SOA production from traditional precursors (Koo et al., 2003; Strader et al., 1999; Weitkamp et al., 2007). In this work, SOAM II was further updated with recently measured higher SOA yields for the low- NO_x photo-oxidation of aromatics (Ng et al., 2007). This update will maximize the calculated SOA contribution from traditional precursors.

Following the approach of Weitkamp et al. (2007), SOAM II was implemented as a box model which considers 13 lumped precursor species that represent 67 individual aromatic, alkane and alkene VOCs. The model uses the measured decay of these precursors to generate condensable products; the partitioning of these products is calculated using absorptive partitioning theory under the assumption that the species are in equilibrium with the wall-loss corrected total aerosol mass concentration (Weitkamp et al., 2007).

We directly measured the decay of 10 traditional SOA precursors with the PTR-MS and GC-MS systems. This included major aromatic and biogenic precursors such as benzene, toluene, ethylbenzene, m- and o-xylenes and α -pinene. Concentrations of other, minor SOA precursors were estimated by using emission ratios with both

Title Page

Abstract

Introduction

Conclusions

References

Tables

Figures

◀

▶

◀

▶

Back

Close

Full Screen / Esc

Printer-friendly Version

Interactive Discussion



toluene and organic carbon emission factors from a published pine wood-combustion emission profile (Schauer et al., 2001). A comparison of emission ratios of compounds we measured indicates that this is a reasonable assumption. For example, Schauer's benzene-to-toluene emission ratio of 2.4 and methacrolein-to-toluene emission ratio of 0.15 are reasonably consistent with our campaign-average values of 4.8 and 0.12, respectively. In some cases, unambiguous identification of a precursor was not possible – for example, xylenes, ethylbenzenes and benzaldehyde all appear at mass 107 in the PTR-MS and were not all separately calibrated-for in the GC-MS. In such cases, VOC concentrations were attributed to the species with the higher SOA yields to give a conservative, upper-limit estimate for SOA production.

3 Experimental results

3.1 Production of Organic Aerosol

Figure 1 shows time-series of results from a typical aging experiment. Figure 1a plots the measured organic aerosol concentration (C_{OA}) and an estimate of the POA mass based on the initial C_{OA} and the wall-loss rate determined from the BC data. There is clear evidence of substantial production of OA. During the first hour of photo-oxidation, the production rate was greater than wall-loss rate and the C_{OA} increased by a factor of 1.3. After about an hour aerosol production slows and absolute concentrations in the chamber fall due to wall loss. Particle size distributions measured with the SMPS are shown in Fig. 2. Before aging, the mass mode was around 90 nm; after aging for four hours, it was about 190 nm. The increase in the particle size was primarily driven by condensational growth.

Figure 1b shows a time series of the total wall-loss-corrected OA. There is good agreement between the BC- and SMPS-based approaches. The initial POA concentration in this experiment was $50 \mu\text{g m}^{-3}$; photo-oxidation increased the total wall-loss-corrected OA to approximately $130 \mu\text{g m}^{-3}$. These levels are consistent with near-

Laboratory studies of the atmospheric aging of wood smoke

A. P. Grieshop et al.

Title Page

Abstract

Introduction

Conclusions

References

Tables

Figures



Back

Close

Full Screen / Esc

Printer-friendly Version

Interactive Discussion



source conditions and concentrations observed in concentrated plumes in the free troposphere associated with long-range continental-scale transport of plumes from intense wildfires (e.g. $OM > 75 \mu\text{g m}^{-3}$ after 1000s of km in; Peltier et al., 2007). The AMS measurements indicate that the dominant component of both the primary and secondary aerosol is organic material, with minor contributions from nitrate (equivalent to 1–5% of the organic mass), ammonium (0.5 to 2% of the organic mass) and chloride (<1% of organic mass).

Figure 1c shows the relative change in gas-phase species measured with the PTR-MS. For example, m/z 81 is associated with monoterpenes and rapidly decays to background levels within an hour. Benzene is detected at m/z 79 by the PTR-MS; it decays very slowly during photo-oxidation. As discussed below, the decay of these and other traditional SOA precursors cannot explain the generation of OA observed in these experiments. Although the gas-phase measurements were primarily used to quantify the decay of known SOA precursors, Fig. 1c also shows a few other PTR-MS fragments that exhibited large changes in multiple experiments. In all experiments, photo-oxidation substantially increased the PTR-MS signals at m/z 31 (formaldehyde), 46 (nitric acid), 47 (formic acid), and 59 (acetone, propanol, methyl vinyl ether, glyoxal or 2,3-butanedione). All of these tentative species designations are based upon instrument inter-comparison studies conducted with biomass-burning emissions, e.g. (Christian et al., 2004; Karl et al., 2007). Across the set of experiments, the PTR-MS signal at m/z 31 increased by a factor of 1.5 to 2.1; the signals at m/z 46 and m/z 47 increased between 2.5 and 7.5 times; and the signal at m/z 59 increased by a factor of 1.2 to 2.2 times. Other masses showing enhancement in more than one experiment were m/z 43 (potentially propene, but also CH_3CO^+ and C_3H_7^+ fragments (Christian et al., 2004)), 45 (acetaldehyde) and 61 (acetic acid and glycolaldehyde). Acetic acid production was observed downwind of African savannah fires (Hobbs et al., 2003) but not in plumes from boreal fires (de Gouw et al., 2006) and is not predicted by photochemical plume models (Trentmann et al., 2005).

Measured O_3 , NO_x and CO concentrations are shown in Fig. 1d. O_3 levels in this

**Laboratory studies of
the atmospheric
aging of wood smoke**A. P. Grieshop et al.

Title Page

Abstract

Introduction

Conclusions

References

Tables

Figures

◀

▶

◀

▶

Back

Close

Full Screen / Esc

Printer-friendly Version

Interactive Discussion



experiment increased by about 200 ppb and NO_x concentration dropped from 63 to 35 ppb during aging. These changes are qualitatively consistent with both field measurements (Hobbs et al., 2003) and model predictions (Trentmann et al., 2003). The ozone concentrations are somewhat higher than might be seen in a real plume due to the lack of continued dilution in the chamber. CO is often used as tracer in plume measurements; Fig. 1d indicates that CO levels were constant throughout the experiment. Hydroxyl radical (OH) concentrations were inferred from the measured decay of multiple light aromatics and published kinetics data. The estimated average concentration was $4(\pm 3) \times 10^6$ molecules cm^{-3} , comparable to daytime conditions in the summer. OH concentrations were reasonably constant throughout the experiment. Therefore, on the basis of observed photochemical activity and mass loading, the experiment conditions are representative of daytime aging of a high-concentration biomass-burning plume.

Figure 1a and b shows an estimate of traditional SOA based on measured precursor decay and SOAM II. Traditional SOA only explained 15% of the observed OA increase. Light aromatics were the most important traditional precursors, contributing 70% of the predicted SOA mass. As illustrated in Fig. 1c, the oxidation rate of light aromatics was much too slow to explain the rapid initial increase in OA concentrations. For example, initial benzene concentration in this experiment was 4 ppb but only 13% of it was oxidized after 5.5 h of aging. The initial toluene concentration was 1 ppb but only 30% of it was oxidized during this experiment. Monoterpenes contributed only 20% of the predicted SOA formation. It is highly unlikely that uncertainty in SOA yields from traditional precursor could explain the large amounts of unaccounted-for OA production.

Substantial OA production was observed in multiple experiments. Figure 3 compiles OA ER calculated using the BC approach for six different experiments. Excluding one high NO_x experiment discussed below, OA ER ranged between 1.8 and 2.7 after 4 to 6 hours of aging. These estimates also agree with results from spectral decomposition of the AMS data¹. The estimated campaign-average OH concentration was $3.6(\pm 0.5) \times 10^6$ molecules cm^{-3} (\pm standard deviation of experiment mean estimates); levels that are representative of typical daytime conditions during the summer. O_3 pro-

Laboratory studies of the atmospheric aging of wood smoke

A. P. Grieshop et al.

Title Page

Abstract

Introduction

Conclusions

References

Tables

Figures

◀

▶

◀

▶

Back

Close

Full Screen / Esc

Printer-friendly Version

Interactive Discussion



duction was a consistent feature and occurred throughout the “lights-on” period during each experiment. Figure 3 indicates that, in some experiments, OA production continued after the UV lights were turned off, potentially through ozone chemistry, as ozone levels declined after the lights were turned off (first order decay of 0.24 ± 0.16 ppb hr^{-1}).

As is summarized in Table 1, the traditional SOA is predicted to contribute only a small fraction of the observed OA production in all experiments. Over the five low- NO_x experiments, modeled SOA production represents an average of 17% of the total SOA production (range 5–30%).

Figure 3 plots data from experiments that aged diluted emissions from soft- and hardwood fires that burned under different combustion conditions. Table 1 summarizes the experimental conditions. Modified combustion efficiencies (MCE; Koppmann et al., 2005) ranged between 0.69 and 0.95 with a median value of 0.91. Reid et al. (2005) uses an MCE value of 0.9 to differentiate between flaming (high MCE) and smoldering (lower MCE) combustion; based on this definition, two of these experiments were performed with emissions from smoldering combustion while the other four were from flaming combustion. OC-to-EC ratios also depend on combustion conditions. The smoldering combustion experiments are OC-dominated while flaming combustion produces substantially more EC. Although experiments were conducted with different fuels and combustion conditions, we did not see any general correlation between OA production and MCE or OC-to-EC ratio.

The conditions of these experiments appear to be reasonably comparable to data from field measurements of biomass plumes. For example, CO/CO_2 mass emission ratios in our experiments range from 5 to 45% with a median of 10% versus a range between 2 and 20% reported by field studies (Koppmann et al., 2005). Table 1 indicates that our OC-to-EC ratio ranged from 1.1 to 13, with lower values associated with flaming combustion (high MCE values) and larger values associated smoldering fires (low MCE values). Field studies report OC-to-EC ratios ranging from 1.7 to 17.3 (Reid et al., 2005) though 5 to 8 are more typical (Andreae and Merlet, 2001). The average NO_x emission ratio for our experiments was $4 (\pm 1) \times 10^{-4}$ $\text{kg NO} (\text{kg CO}_2)^{-1}$,

**Laboratory studies of
the atmospheric
aging of wood smoke**A. P. Grieshop et al.

[Title Page](#)[Abstract](#)[Introduction](#)[Conclusions](#)[References](#)[Tables](#)[Figures](#)[◀](#)[▶](#)[◀](#)[▶](#)[Back](#)[Close](#)[Full Screen / Esc](#)[Printer-friendly Version](#)[Interactive Discussion](#)

**Laboratory studies of
the atmospheric
aging of wood smoke**

A. P. Grieshop et al.

Title Page

Abstract

Introduction

Conclusions

References

Tables

Figures

◀

▶

◀

▶

Back

Close

Full Screen / Esc

Printer-friendly Version

Interactive Discussion



which is on the low end of field data (Andreae and Merlet, 2001). The campaign primary OC emission factor (assuming an OM:OC ratio of 2.1 (Turpin and Lim, 2001)) was $0.7 \pm 1.0 \text{ g C (kg CO}_2\text{)}^{-1}$ (average \pm standard deviation) which is also somewhat lower than field data (Andreae and Merlet, 2001). However, OC emissions measured in source tests may be biased high due to sample collection at high C_{OA} influencing the gas-particle partitioning of semivolatile organic compounds (Lipsky and Robinson, 2006; Shrivastava et al., 2006) and because many studies do not account for filter sampling artifacts (Subramanian et al., 2004). Ratios of benzene and toluene with CO (shown in Table 1) were quite variable, but generally show reasonable agreement with values from literature (de Gouw et al., 2006). The acetonitrile-to-CO ratios measured were a factor of 2 to 10 lower than most literature values.

Much less OA was produced in one experiment in which 220 ppbv of NO was added to the chamber before turning on the UV lights. This experiment is labeled as high NO_x in Fig. 3. The chemistry for this experiment appeared to be fundamentally different than any of the other experiments. After adding the NO, O_3 concentration dropped for about an hour indicating titration. In addition, Fig. 3 shows that the OA ER initially decreased after the lights were turned on, presumably due to evaporation. This suggests that OA production from photo-oxidation of wood smoke depends on the VOC-to- NO_x ratio. Such dependence has been observed for traditional SOA precursors due to peroxy radical chemistry (Ng et al., 2007; Presto et al., 2005b). However, NO_x levels in this experiment are likely much higher than typical fire plumes: the NO_x -to-benzene and toluene ratios in this experiment were a factor of 5–100 higher than typical plumes (Andreae and Merlet, 2001). In addition, chamber CO and CO_2 levels were also much lower during this experiment, which potentially indicates there may have been a problem with the sampling.

3.2 Organic Aerosol Volatility

The volatility of the OA was measured with the thermodenuder (TD). The SMPS size distributions shown in Fig. 2 indicate that the passing both the fresh and aged aerosol

through the TD substantially reduced particle volume, especially for the fresh emissions. To quantify the changes in aerosol mass with temperature, Fig. 4a shows the MFR of fresh and aged OA measured with the AMS as a function of TD temperature (a plot referred to here as a thermogram).

5 Figure 4a indicates that between 50% and 80% percent of fresh POA evaporated at 50°C. Therefore, the majority of wood smoke POA should be classified as semivolatile at typical atmospheric conditions, consistent with recent dilution sampler (Lipsky and Robinson, 2006; Shrivastava et al., 2006) and thermal denuder measurements³. For example, Huffman et al.³ report that POA in emissions from 9 of the 15 different biomass samples lost 50% or more of their mass at a TD temperature below 100°C.

10 The aged OA was always less volatile than freshly emitted POA. For example, Fig. 4a indicates that only 20 to 40% of the aged OA mass evaporated at 50°C in our TD. Such a shift is consistent with photo-oxidation creating more oxygenated but less volatile compounds. For example, the AMS m/z 44 signal increases during aging, indicating that the OA is becoming progressively more oxygenated¹. However, it is counter to current treatments of OA in chemical transport models, which assume that POA is non-volatile and that SOA is semivolatile (Shrivastava et al., 2008). Recent TD measurements of both ambient and biomass burning aerosols suggest a similar conclusion³.

20 Figure 5 shows the time series of OA MFR at 50°C measured during several experiments. In every experiment, the OA volatility decreased substantially during the first hour of photo-oxidation, but then remained essentially constant with subsequent aging. This step-change-like behavior means that the OA formed during the initial stages of photo-oxidation is much less volatile than the POA. However, a step change in volatility is somewhat surprising considering that there was sustained production of OA in every experiment (Fig. 3) and that the AMS data indicates that OA becomes more progres-

25 ³Huffman, J. A., Aiken, A. C. Docherty, K. S., Ulbrich, I. M., DeCarlo, P. F., Jayne, J. T., Onasch, T. B., Trimborn, A., Worsnop, D. R., Ziemann, P. J., and Jimenez, J. L.: Volatility of primary and secondary organic aerosols in the field contradicts current model representations, Environ. Sci. Technol., submitted, 2008

Laboratory studies of the atmospheric aging of wood smoke

A. P. Grieshop et al.

[Title Page](#)[Abstract](#)[Introduction](#)[Conclusions](#)[References](#)[Tables](#)[Figures](#)[⏪](#)[⏩](#)[◀](#)[▶](#)[Back](#)[Close](#)[Full Screen / Esc](#)[Printer-friendly Version](#)[Interactive Discussion](#)

sively more oxygenated as the experiment progresses¹. Somehow the changes that occurred after about an hour of photo-oxidization did not alter the observed overall OA volatility.

An uncertainty when interpreting TD data is whether or not the aerosol has reached equilibrium given its limited residence time inside the heated section of the TD (An et al., 2007). If the OA is not in equilibrium then the TD underestimates its volatility; under these conditions the TD is measuring relative evaporation rates, which depend on particle size (Seinfeld, 1998). The increase in particle size due to condensational growth will slow evaporation, potentially biasing our interpretation that the aged OA is less volatile than fresh OA. A dynamic mass transfer model of the aerosol in the TD indicates that the measured changes in particle size were insufficient to cause a substantial change in particle equilibration time (Stanier et al., 2007). We suggest two potential explanations for the step-change in particle volatility:

1. time-varying OA composition (as discussed above); or
2. evolving kinetic limitations, either due to accommodation at the particle surface or other uptake processes, which limit the evaporation of the bulk aerosol.

As described in the companion paper¹, TD data for individual AMS fragments provides some support for the latter explanation, but further investigation is needed.

4 Basis-set modeling

As previously discussed, traditional SOA cannot explain the large production of OA observed in these experiments. In this section we compare our data to predictions of the model of Robinson et al. (2007) to investigate the hypothesis that the unaccounted for OA production is due to oxidation of low-volatility organic vapors. This hypothesis is motivated by several pieces of evidence. Wood smoke contains thousands of individual organic compounds, distributed across a wide range of volatilities. Source dilution

Laboratory studies of the atmospheric aging of wood smoke

A. P. Grieshop et al.

Title Page

Abstract

Introduction

Conclusions

References

Tables

Figures

◀

▶

◀

▶

Back

Close

Full Screen / Esc

Printer-friendly Version

Interactive Discussion



experiments have shown that a large fraction of wood smoke POA evaporates upon isothermal dilution (Lipsky and Robinson, 2006; Shrivastava et al., 2006). Therefore, a substantial pool of low-volatility organic vapors exist in plumes (and our chamber). Oxidation of these vapors will produce acids, nitrates, and carbonyls, which have lower vapor pressures than the parent compounds (Pankow and Asher, 2008). Given the low initial volatility of the parent compounds, we expect oxidation of these vapors to form OA with high efficiency; for example, SOA yields from n-alkanes increase with carbon number (Lim and Ziemann, 2005).

The model is described in detail by Robinson et al. (2007) and Shrivastava et al. (2008). Table 3 summarizes the input parameters, most of which are from Robinson et al. (2007). The model is based on the volatility basis-set framework (Donahue et al., 2006), which was implemented in a box model. The model tracks the concentration of low-volatility organics using a nine-bin volatility basis set; the bins have effective saturation concentrations (C^*) that are distributed between 0.01 and $10^6 \mu\text{g m}^{-3}$ at 298 K. Gas-particle partitioning is calculated using absorptive partitioning theory (Pankow, 1994) assuming that all of the organics form a quasi-ideal solution and that the bulk gas and particle phases are in equilibrium.

The initial concentration in each bin was determined based on the measured POA concentrations and an assumed volatility distribution. We consider the two volatility distributions proposed by Robinson et al. (2007) to represent the POA emissions (separate simulations are done with each distribution). These distributions are shown in Fig. 6a; one distribution is based on the partitioning measurements of the organics collected on quartz filters and the second includes additional emissions of intermediate volatility organic compounds (IVOCs) that are presumably not captured on the quartz filters.

Figure 6b examines the suitability of applying these distributions, which are based on diesel exhaust data, to represent wood smoke. The curves plotted show the gas-particle partitioning for the two volatility distributions vary as a function of C_{OA} . Also shown in Fig. 6b are gas-particle partitioning data for wood smoke measured with

**Laboratory studies of
the atmospheric
aging of wood smoke**A. P. Grieshop et al.

Title Page

Abstract

Introduction

Conclusions

References

Tables

Figures

◀

▶

◀

▶

Back

Close

Full Screen / Esc

Printer-friendly Version

Interactive Discussion



dilution samplers (Lipsky and Robinson, 2006; Shrivastava et al., 2006). The predicted gas-particle partitioning based on either distribution agrees well with the experimental data, justifying their use in our simulations. It also supports the approach of Robinson et al. (2007) to use one distribution to represent all POA emissions.

After determining the initial concentrations of low-volatility organics, the model simulates aging by reacting the vapors with OH. Following Robinson et al. (2007), the OH reaction rate constant (k_{OH}) is $4 \times 10^{-11} \text{ cm}^3 \text{ molec}^{-1} \text{ s}^{-1}$ (slightly higher than that expected for the OH oxidation of a large n-alkane) and the scheme assumes a modest (7.5%) net increase in mass per reaction to account for added oxygen (equivalent to adding a single oxygen atom to a C_{15} alkane). Each reaction reduces the volatility of the vapors by a factor of ten (i.e. shifts the material to the next lower volatility bin), which changes the gas-particle partitioning and creates new OA. The aging mechanism is driven by the OH concentrations inferred from the measured decay of several VOCs.

Figure 7a compares the OA ER predicted by the Robinson et al. (2007) aging mechanism to the average measured value for the five low- NO_x experiments. The measured ER shown in Fig. 7a has been corrected for predicted SOA from traditional precursors; therefore it only represents the unaccounted-for OA production. The simulation using the filter-only volatility distribution reproduces the measured OA production. The fact that this model predicts the magnitude of the production is not surprising since the dilution sampler data plotted in Fig. 6b indicate that under the conditions of a typical experiment (initial $\text{C}_{\text{OA}} \sim 100 \mu\text{g m}^{-3}$) there are sufficient low-volatility vapors to double or triple the OA concentrations.

Figure 7a indicates the model based on the filter-plus-IVOC volatility distribution outpaces the observed production after about 2 h of aging. Likely explanations are that this model overestimates the concentrations of IVOC vapors and/or that the aging mechanism is not appropriately altering the volatility distribution. The comparisons in Shrivastava et al. (2008) suggest that wood combustion emits relatively less IVOCs than motor vehicles, lending support to the first concern. Furthermore, the aging mecha-

**Laboratory studies of
the atmospheric
aging of wood smoke**A. P. Grieshop et al.

[Title Page](#)[Abstract](#)[Introduction](#)[Conclusions](#)[References](#)[Tables](#)[Figures](#)[◀](#)[▶](#)[◀](#)[▶](#)[Back](#)[Close](#)[Full Screen / Esc](#)[Printer-friendly Version](#)[Interactive Discussion](#)

nism assumes that the reaction products all have lower volatility than the precursors; this assumption likely breaks down after the multiple generations of processing that are required to transfer IVOC vapors into the condensed phase.

Figure 7a indicates that none of the models reproduce the detailed dynamics of the OA production rate. For example, all of the experiments show an initial rapid burst of OA production that slows after about an hour or so of aging, a behavior which is not captured by the model.

The OA composition measured with the AMS can also be used to evaluate the basis-set model. As described in a companion paper¹, the AMS data indicate that aging continuously increases the amount of oxygenated OA. Aiken et al. (2008) define a relationship to estimate the OA O:C ratio based on the AMS signal at m/z 44 (CO_2^+). Figure 7b shows the average O:C ratio calculated for the five low- NO_x experiments (see Grieshop et al., 2008¹ for further discussion of the AMS data). Also plotted in Fig. 7b is the modeled O:C as a function of age. Results are only shown for the volatility distribution based on the filter data because the addition of IVOCs to the distribution minimally affected the predicted O:C ratio. The initial condition for this calculation is the estimated experiment average O:C ratio (0.32) of the POA. The model then tracks the added oxygen, based on the assumed 7.5% increase in mass per generation. The base Robinson et al. (2007) model only increases the predicted O:C ratio from 0.32 to 0.38 after 4 h of aging versus an average measured increase of 0.32 to 0.48. Therefore, it does not add enough oxygen to the OA.

To determine if the observed changes in O:C ratio can be plausibly reproduced by this aging mechanism, the model parameters were slightly modified. The modified model reduces the volatility of gas-phase material by a factor of 100 with each generation of oxidation (a two bin shift), the OH reaction rate was halved to $2 \times 10^{-11} \text{ cm}^3 \text{ molec}^{-1} \text{ s}^{-1}$ and the organic mass was increased by 40% for each generation of oxidation (equivalent to adding about 5 oxygen atoms to a C_{15} alkane). As shown in Fig. 7a these modifications have little effect on the predicted OA enhancement; however, they improve the predictions of OA oxygen content. A reduction of C*

**Laboratory studies of
the atmospheric
aging of wood smoke**A. P. Grieshop et al.

[Title Page](#)[Abstract](#)[Introduction](#)[Conclusions](#)[References](#)[Tables](#)[Figures](#)[⏪](#)[⏩](#)[◀](#)[▶](#)[Back](#)[Close](#)[Full Screen / Esc](#)[Printer-friendly Version](#)[Interactive Discussion](#)

by a factor of 100 per generation oxidation is supported by the effects on volatility of additional molecular functionality (Pankow and Asher, 2008). However, the amount of added oxygen per generation is somewhat higher than what would be expected; for example, the mechanism of Lim and Ziemann (2005) adds up to four oxygen atoms per generation. A potential explanation is that fragmentation reactions that break the carbon backbone may play an important role in the photochemical aging of primary emissions. Reducing the size of the carbon backbone will lead to more rapid increases in O:C while also limiting the overall OA growth due to volatilization of the lighter fragments. It thus has the potential to explain the sharp initial increase in OA, the sharp initial decrease in volatility, and the progressive increase in particle-phase O:C.

The OA volatility measurements made with the TD provide a final test of the model. In order to compare the model predictions to the data, the calculated volatility distributions were analyzed with a TD model that is similar to that used by Stanier et al. (2007). The TD model calculates the MFR of a multi-component organic particle as a function of temperature and TD residence time. It uses the Clausius-Clapeyron equation to calculate the effects of temperature on C^* . Table 3 lists the enthalpies of vaporization and molecular weights for this calculation; they are based on data for large saturated species commonly found in primary emissions (Donahue et al., 2006). The other key input parameter for the TD model is the uptake coefficient. We term this an uptake coefficient here because it is unclear whether mass accommodation (which would call for the use of an accommodation coefficient) or some other process is limiting the particle evaporation rate. Figure 4b compares measured and predicted OA MFR as a function of temperature for both fresh and aged OA. Results are only shown for the modified set of input parameters; results for the base model with the filter-only distribution are similar to these predictions. If the TD model uses an uptake coefficient of one (which means that the OA has reached equilibrium at the end of the TD), Figs. 4b and 7c indicate that the model over-predicts the extent of OA evaporation. Figure 7c shows that much better agreement is observed if the uptake coefficient is reduced to 0.05 or 0.01. Recent studies report that similarly small uptake coefficients are required to reproduce

**Laboratory studies of
the atmospheric
aging of wood smoke**A. P. Grieshop et al.

[Title Page](#)[Abstract](#)[Introduction](#)[Conclusions](#)[References](#)[Tables](#)[Figures](#)[◀](#)[▶](#)[◀](#)[▶](#)[Back](#)[Close](#)[Full Screen / Esc](#)[Printer-friendly Version](#)[Interactive Discussion](#)

**Laboratory studies of
the atmospheric
aging of wood smoke**

A. P. Grieshop et al.

[Title Page](#)[Abstract](#)[Introduction](#)[Conclusions](#)[References](#)[Tables](#)[Figures](#)[⏪](#)[⏩](#)[◀](#)[▶](#)[Back](#)[Close](#)[Full Screen / Esc](#)[Printer-friendly Version](#)[Interactive Discussion](#)

the measured evaporation rates of SOA (Grieshop et al., 2007; Stanier et al., 2007) and POA⁴ volatility. The experimental data can also be reproduced by assuming an uptake coefficient of one and using very small (and physically unrealistic) enthalpies of vaporization. This second approach has been used to parameterize aerosol volatility (Pathak et al., 2007; Stanier et al., 2007); however, we believe an uptake coefficient that is less than one is more physically justifiable than an enthalpy of vaporization less than about 50 kJ mol⁻¹. More research is needed to address these issues, but this is beyond the scope of this paper.

Figure 7c shows campaign-average MFR data at 50°C as a function of aging time along with output from the coupled aging and TD models. We only show results for the modified set of input parameters for three different uptake coefficients. Results for the other sets of input parameters are similar to these. The predicted MFRs show that the aging mechanism progressively reduces the OA volatility, consistent with the experimental data. However, the model predicts that the extent of particle evaporation decreases continuously with increasing age while the experimental data shows a step change. Limitations in our understanding of evaporation kinetics restrict our ability to make quantitative comparisons between the measured and predicted MFRs. However, the model predictions are at least qualitatively consistent with the observed shift in volatility.

5 Discussion and Conclusions

Photo-oxidation of diluted wood combustion emissions in a smog chamber rapidly produces substantial OA, greatly in excess of what can be explained by the measured decay of traditional SOA precursors. The rate and magnitude of the OA production in our experiments is consistent with field observations of aerosol mass production down-

⁴Grieshop, A. P. and Robinson, A. L.: Gas-particle partitioning of fresh diesel emissions at near-ambient concentrations, in preparation, 2008.

wind of large fires (Reid et al., 2005). For example, Lee et al. (2008) report 1.5 to 6-fold enhancements of OA concentrations after 3 to 4 h of aging downwind of a prescribed burn in Georgia. Substantial OA production downwind of fires may help explain carbon-isotope studies indicating that modern carbon is often the dominant contributor to OA, even in urban areas (Hildemann et al., 1994; Szidat et al., 2006; Tanner et al., 2004; Zheng et al., 2006).

Field studies have attributed OA production in fire plumes to slow condensation of large hydrocarbons (Reid et al., 1998), enhanced isoprenoid emissions (Lee et al., 2008), and acid-catalyzed reactions (Nopmongkol et al., 2007). Given the complexity of these experiments, which feature actual emissions with pre-existing aerosol and a complex mixture of gas-phase compounds at plume-like conditions, it is difficult to identify the source of the unexplained OA. We attribute the production of the unexplained OA to the oxidation of low-volatility organic vapors. Dilution sampler measurements indicate that large hydrocarbons do not condense but evaporate as the plume continues to isothermally disperse at atmospheric temperatures (Lipsky and Robinson, 2006; Shrivastava et al., 2006). Fires do emit isoprenoid such as monoterpenes, but in our experiments these emissions were almost two orders of magnitude too low to explain the observed OA production. Finally, the lack of inorganic acidity likely reduces the potential for acid-catalyzed reactions in our experiments.

The reasonable agreement between the measured OA production and predictions of the model of Robinson et al. (2007) indicate that the large excess OA formed in our experiments can be explained by photo-oxidation of low-volatility organic vapors. This is the same conclusion reached in our recent work with diesel exhaust (Robinson, 2007; Sage et al., 2008; Weitkamp et al., 2007). In fact, the similarity between these results and our previous work with diesel exhaust is striking. It underscores the fact that most combustion systems emit substantial amounts of low-volatility organics that exist as vapors at typical atmospheric conditions. In fact, the concentrations of these vapors appear to greatly exceed POA at atmospheric conditions (Lipsky and Robinson, 2006; Shrivastava et al., 2008; Shrivastava et al., 2006; Grieshop and Robinson,

**Laboratory studies of
the atmospheric
aging of wood smoke**A. P. Grieshop et al.

[Title Page](#)[Abstract](#)[Introduction](#)[Conclusions](#)[References](#)[Tables](#)[Figures](#)[◀](#)[▶](#)[◀](#)[▶](#)[Back](#)[Close](#)[Full Screen / Esc](#)[Printer-friendly Version](#)[Interactive Discussion](#)

2008⁴, consistent with the observed doubling or tripling OA concentrations after moderate amounts of aging of diluted emissions in a smog chamber. A challenge is that the chemical identity of the vast majority of low-volatility organics is not known because they appear as an unresolved complex mixture (UCM) in traditional gas chromatographic analysis (Schauer et al., 2001). The volatility basis-set approach provides a semi-empirical framework to treat the partitioning and aging of this complex mixture. The success of the basis-set model in simulating these experiments is encouraging, but the model-measurement comparison indicates that more research is needed to accurately represent the volatility and aging of primary emissions. Important uncertainties include the treatment of IVOCs, fragmentation in the aging mechanism, and the rapid increases in OA oxygen content.

The thermodenuder data provide new insight into OA volatility. They demonstrate that fresh POA is more volatile than the aged OA produced from photo-oxidation. This is in contrast to the current treatment in chemical transport models, which assumes that POA is non volatile and SOA is semivolatile. Analysis of recent thermodenuder measurements of ambient OA reached a similar conclusion³. Photo-oxidation adds functionality (nitrate, carbonyl, acid groups, etc.) creating compounds with substantially lower volatility than the original species (Pankow and Asher, 2008). The fact that the aged OA is less volatile than the POA supports the conclusion that oxidation of low-volatility organic vapors is an important source of OA as opposed to oxidation of traditional, very volatile SOA precursors. Oxidation of low-volatility vapors creates products with even lower volatilities, potentially much lower than semivolatile POA and traditional SOA formed from very volatile precursors.

Acknowledgements. This research was supported by the EPA STAR program through the National Center for Environmental Research (NCER) under grants R833748. This paper has not been subject to EPA's required peer and policy review, and therefore does not necessarily reflect the views of the Agency. No official endorsement should be inferred. The PTR-MS and AMS were acquired with support from the NSF (ATM-0420842). The authors gratefully acknowledge Jose-Luis Jimenez for comments on a draft manuscript and Manish Shrivastava

**Laboratory studies of
the atmospheric
aging of wood smoke**A. P. Grieshop et al.

[Title Page](#)[Abstract](#)[Introduction](#)[Conclusions](#)[References](#)[Tables](#)[Figures](#)[⏪](#)[⏩](#)[◀](#)[▶](#)[Back](#)[Close](#)[Full Screen / Esc](#)[Printer-friendly Version](#)[Interactive Discussion](#)

and Jeffrey Pierce for assistance with model configuration.

References

- Abel, S. J., Haywood, J. M., Highwood, E. J., Li, J., and Buseck, P. R.: Evolution of biomass burning aerosol properties from an agricultural fire in southern Africa, *Geophys. Res. Lett.*, 30(15), 1783, doi:10.1029/2003GL017342, 2003.
- Aiken, A. C., DeCarlo, P. F., Kroll, J. H., Worsnop, D. R., Huffman, J. A., Docherty, K. S., Ulbrich, I. M., Mohr, C., Kimmel, J. R., Sueper, D., Sun, Y., Zhang, Q., Trimborn, A., Northway, M., Ziemann, P. J., Canagaratna, M. R., Onasch, T. B., Alfarra, M. R., Prevot, A. S. H., Dommen, J., Duplissy, J., Metzger, A., Baltensperger, U., and Jimenez, J. L.: O/C and OM/OC Ratios of Primary, Secondary, and Ambient Organic Aerosols with High-Resolution Time-of-Flight Aerosol Mass Spectrometry, *Environ. Sci. Technol.*, 2(12), 4478–4485, 2008.
- An, W. J., Pathak, R. K., Lee, B., and Pandis, S. N.: Aerosol volatility measurement using an improved thermodenuder: application to secondary organic aerosol, *J. Aerosol Sci.*, 38(2), 305–314, 2007.
- Andreae, M. O. and Merlet, P.: Emission of trace gases and aerosols from biomass burning, *Global Biogeochem. Cy.*, 15(4), 955–966, 2001.
- Andreae, M. O., Rosenfeld, D., Artaxo, P., Costa, A. A., Frank, G. P., Longo, K. M., and Silva-Dias, M. A. F.: Smoking rain clouds over the Amazon, *Science*, 303(5662), 1337–1342, 2004.
- Bond, T. C., Streets, D. G., Yarber, K. F., Nelson, S. M., Woo, J. H., and Klimont, Z.: A technology-based global inventory of black and organic carbon emissions from combustion, *J. Geophys. Res.-Atmos.*, 109(D14), D14203, doi:10.1029/2003JD003697, 2004.
- Canagaratna, M. R., Jayne, J. T., Jimenez, J. L., Allan, J. D., Alfarra, M. R., Zhang, Q., Onasch, T. B., Drewnick, F., Coe, H., Middlebrook, A., Delia, A., Williams, L. R., Trimborn, A. M., Northway, M. J., DeCarlo, P. F., Kolb, C. E., P. Davidovits, and Worsnop, D. R.: Chemical and microphysical characterization of ambient aerosols with the aerodyne aerosol mass spectrometer, *Mass Spectrom. Rev.*, 26(2), 185–222, 2007.
- Carter, W., Cocker, D., Fitz, D., Malkina, I., Bumiller, K., Sauer, C., Pisano, J., Bufalino, C., and Song C.: A new environmental chamber for evaluation of gas-phase chemical mechanisms and secondary aerosol formation, *Atmos. Environ.*, 39(40), 7768–7788, 2005.

Laboratory studies of the atmospheric aging of wood smoke

A. P. Grieshop et al.

Title Page

Abstract

Introduction

Conclusions

References

Tables

Figures

◀

▶

◀

▶

Back

Close

Full Screen / Esc

Printer-friendly Version

Interactive Discussion



**Laboratory studies of
the atmospheric
aging of wood smoke**A. P. Grieshop et al.

[Title Page](#)[Abstract](#)[Introduction](#)[Conclusions](#)[References](#)[Tables](#)[Figures](#)[◀](#)[▶](#)[◀](#)[▶](#)[Back](#)[Close](#)[Full Screen / Esc](#)[Printer-friendly Version](#)[Interactive Discussion](#)

Christian, T. J., Kleiss, B., Yokelson, R., Holzinger, J. R., Crutzen, P. J., Hao, W. M., Shirai, T., and Blake, D. R.: Comprehensive laboratory measurements of biomass-burning emissions – 2: First intercomparison of open-path FTIR, PTR-MS, and GC-MS/FID/ECD, *J. Geophys. Res.-Atmos.*, 109(D2), D02311, doi:10.1029/2003JD003874, 2004.

5 Crosier, J., Jimenez, J. L., Allan, J. D., Bower, K. N., Williams, P. I., Alfarra, M. R., Canagaratna, M. R., Jayne, J. T., Worsnop, D. R., and Coe, H.: Technical Note: Description and use of the new Jump Mass Spectrum mode of operation for the Aerodyne Quadrupole Aerosol Mass Spectrometers (Q-AMS), *Aerosol Sci. Technol.*, 41(9), 865–872, 2007.

10 de Gouw, J. A., Warneke, C., Stohl, A., Wollny, A. G., Brock, C. A., Cooper, O. R., Holloway, J. S., Trainer, M., Fehsenfeld, F. C., Atlas, E. L., Donnelly, S. G., Stroud, V., and Lueb, A.: Volatile organic compounds composition of merged and aged forest fire plumes from Alaska and western Canada, *J. Geophys. Res.-Atmos.*, 111(D10), D10303, doi:10.1029/2005JD006175, 2006.

15 Donahue, N. M., Robinson, A. L., Stanier, C. O., and Pandis, S. N.: Coupled partitioning, dilution, and chemical aging of semivolatile organics, *Environ. Sci. Technol.*, 40(8), 2635–2643, 2006.

Grieshop, A. P., Donahue, N. M., and Robinson, A. L.: Is the Gas-Particle Partitioning in alpha-Pinene Secondary Organic Aerosol Reversible?, *Geophys. Res. Lett.*, 34, L14810, doi:10.1029/2007GL029987, 2007.

20 Hildemann, L., Klinedinst, D., Klouda, G., Currie, L., and Cass, G.: Sources of Urban Contemporary Carbon Aerosol, *Environ. Sci. Technol.*, 28(9), 1565–1576, 1994.

Hobbs, P. V., Sinha, P., Yokelson, R. J., Christian, T. J., Blake, D. R., Gao, S., Kirchstetter, T. W., Novakov, T., and Pilewskie, P.: Evolution of gases and particles from a savanna fire in South Africa, *J. Geophys. Res.-Atmos.*, 108(D13), 8485, doi:10.1029/2002JD002352, 2003.

25 Karl, T. G., Christian, T. J., Yokelson, R. J., Artaxo, P., Hao, W. M., and Guenther, A.: The Tropical Forest and Fire Emissions Experiment: method evaluation of volatile organic compound emissions measured by PTR-MS, FTIR, and GC from tropical biomass burning, *Atmos. Chem. Phys.*, 7, 5883–5897, 2007, <http://www.atmos-chem-phys.net/7/5883/2007/>.

30 Kirchstetter, T. W. and Novakov, T.: Controlled generation of black carbon particles from a diffusion flame and applications in evaluating black carbon measurement methods, *Atmos. Environ.*, 41(9), 1874–1888, 2007.

Kirchstetter, T. W., Novakov, T., and Hobbs, P. V.: Evidence that the spectral dependence of light

absorption by aerosols is affected by organic carbon, *J. Geophys. Res.-Atmos.*, 109(D21), D21208, doi:10.1029/2004JD004999, 2004.

Koo, B. Y., Ansari, A. S., and Pandis, S. N.: Integrated approaches to modeling the organic and inorganic atmospheric aerosol components, *Atmos. Environ.*, 37(34), 4757–4768, 2003.

5 Koppmann, R., von Czapiewski, K., and Reid, J. S.: A review of biomass burning emissions – Part 1: gaseous emissions of carbon monoxide, methane, volatile organic compounds, and nitrogen containing compounds, *Atmos. Chem. Phys. Discuss.*, 5, 10455–10516, 2005.

Lee, S., Kim, H. K., Yan, B., Cobb, C. E., Hennigan, C., Nichols, S., Chamber, M., Edgerton, E. S., Jansen, J. J., Hu, Y. T., Zheng, M., Weber, R. J., and Russell, A. G.: Diagnosis of aged prescribed burning plumes impacting an urban area, *Environ. Sci. Technol.*, 42(5), 1438–1444, 2008.

15 Lelieveld, J., Crutzen, P. J., Ramanathan, V., Andreae, M. O., Brenninkmeijer, C. A. M., Campos, T., Cass, G. R., Dickerson, R. R., Fischer, H., de Gouw, J. A., Hansel, A., Jefferson, A., Kley, D., de Laat, A. T. J., Lal, S., Lawrence, M. G., Lobert, J. M., Mayol-Bracero, O. L., Mitra, A. P., Novakov, T., Oltmans, S. J., Prather, K. A., Reiner, T., Rodhe, H., Scheeren, H. A., Sikka, D., and Williams, J.: The Indian Ocean Experiment: Widespread air pollution from South and Southeast Asia, *Science*, 291, 5506, 1031–1036, 2001.

20 Lim, Y. B. and Ziemann, P. J.: Products and mechanism of secondary organic aerosol formation from reactions of n-alkanes with OH radicals in the presence of NO_x, *Environ. Sci. Technol.*, 39(23), 9229–9236, 2005.

Lipsky, E. M. and Robinson, A. L.: Effects of dilution on fine particle mass and partitioning of semivolatile organics in diesel exhaust and wood smoke, *Environ. Sci. Technol.*, 40(1), 155–162, 2006.

25 Millet, D. B., Donahue, N. M., Pandis, S. N., Polidori, A., Stanier, C. O., Turpin, B. J., and Goldstein, A. H.: Atmospheric volatile organic compound measurements during the Pittsburgh Air Quality Study: Results, interpretation, and quantification of primary and secondary contributions, *J. Geophys. Res.-Atmos.*, 110, D07S07, doi:10.1029/2004JD004601, 2005.

Ng, N. L., Kroll, J. H., Chan, A. W. H., Chhabra, P. S., Flagan, R. C., and Seinfeld, J. H.: Secondary organic aerosol formation from m-xylene, toluene, and benzene, *Atmos. Chem. Phys.*, 7, 3909–3922, 2007,
30 <http://www.atmos-chem-phys.net/7/3909/2007/>.

Nopmongcol, U., Khamwicht, W., Fraser, M. P., and Allen, D. T.: Estimates of heterogeneous formation of secondary organic aerosol during a wood smoke episode in Houston, Texas,

**Laboratory studies of
the atmospheric
aging of wood smoke**

A. P. Grieshop et al.

Title Page

Abstract

Introduction

Conclusions

References

Tables

Figures

◀

▶

◀

▶

Back

Close

Full Screen / Esc

Printer-friendly Version

Interactive Discussion



- Atmos. Environ., 41(14), 3057–3070, 2007.
- Pankow, J. F.: An Absorption-Model of Gas-Particle Partitioning of Organic-Compounds in the Atmosphere, *Atmos. Environ.*, 28(2), 185–188, 1994.
- Pankow, J. F. and Asher, W. E.: SIMPOL.1: a simple group contribution method for predicting vapor pressures and enthalpies of vaporization of multifunctional organic compounds, *Atmos. Chem. Phys.*, 8, 2773–2796, 2008,
5 <http://www.atmos-chem-phys.net/8/2773/2008/>.
- Pathak, R. K., Presto, A. A., Lane, T. E., Stanier, C. O., Donahue, N. M., and Pandis, S. N.: Ozonolysis of alpha-pinene: parameterization of secondary organic aerosol mass fraction, *Atmos. Chem. Phys.*, 7(14), 3811–3821, 2007.
- Peltier, R. E., Sullivan, A. P., Weber, R. J., Brock, C. A., Wollny, A. G., Holloway, J. S., de Gouw, J. A., and Warneke, C.: Fine aerosol bulk composition measured on WP-3D research aircraft in vicinity of the Northeastern United States; results from NEAQS, *Atmos. Chem. Phys.*, 7, 3231–3247, 2007,
10 <http://www.atmos-chem-phys.net/7/3231/2007/>.
- Pierce, J. R., Engelhart, G. J., Weitkamp, E. A., Pathak, R. K., Pandis, S. N., Donahue, N. M., Robinson, A. R., and Adams, P. J.: Constraining particle evolution from wall losses, coagulation, and condensation-evaporation in smog-chamber experiments: optimal estimation based on size distribution measurements., *Aerosol. Sci. Technol.*, in press, 2008.
- Presto, A. A., Huff Hartz, K. E., and Donahue, N. M.: Secondary organic aerosol production from terpene ozonolysis – 1: Effect of UV radiation, *Environ. Sci. Technol.*, 39(18), 7036–7045, 2005a.
- Presto, A. A., Huff Hartz, K. E., and Donahue, N. M.: Secondary organic aerosol production from terpene ozonolysis – 2: Effect of NO_x concentration, *Environ. Sci. Technol.*, 39(18),
20 7046–7054, 2005b.
- Ramanathan, V., Li, F., Ramana, M. V., Praveen, P. S., Kim, D., Corrigan, C. E., Nguyen, H., Stone, E. A., Schauer, J. J., Carmichael, G. R., Adhikary, B., and Yoon, S. C.: Atmospheric brown clouds: hemispherical and regional variations in long-range transport, absorption, and radiative forcing, *J. Geophys. Res.-Atmos.*, 112, D22S21, doi:10.1029/2006JD008124,
25 2007.
- Reid, J., Hobbs, P., Ferek, R., Blake, D., Martins, J., Dunlap, M., and Liousse, C.: Physical, chemical, and optical properties of regional hazes dominated by smoke in Brazil, *J. Geophys. Res.*, 103(D24), 32 059–32 080, 1998.

**Laboratory studies of
the atmospheric
aging of wood smoke**A. P. Grieshop et al.

[Title Page](#)[Abstract](#)[Introduction](#)[Conclusions](#)[References](#)[Tables](#)[Figures](#)[◀](#)[▶](#)[◀](#)[▶](#)[Back](#)[Close](#)[Full Screen / Esc](#)[Printer-friendly Version](#)[Interactive Discussion](#)

Reid, J. S., Koppmann, R., Eck, T. F., and Eleuterio, D. P.: A review of biomass burning emissions part II: intensive physical properties of biomass burning particles, *Atmos. Chem. Phys.*, 5, 799–825, 2005,

<http://www.atmos-chem-phys.net/5/799/2005/>.

5 Robinson, A. L., Donahue, N. M., Shrivastava, M. K., Weitkamp, E. A., Sage, A. M., Grieshop, A. P., Lane, T. E., Pierce, J. R., and Pandis, S. N.: Rethinking Organic Aerosols: Semivolatile Emissions and Photochemical Aging, *Science*, 315, 1259–1262, 2007.

Robinson, A. L., Subramanian, R., Donahue, N. M., Bernardo-Bricker, A., and Rogge, W. F.: Source apportionment of molecular markers and organic aerosol – 2: Biomass smoke, *Environ. Sci. Technol.*, 40(24), 7811–7819, 2006.

10 Sage, A. M., Weitkamp, E., Donahue, N. M., and Robinson, A. L.: Evolving mass spectra of the oxidized component of organic aerosol: Results from aerosol mass spectrometer analyses of aged diesel emissions, *Atmos. Chem. Phys.*, 8, 1139–1152, 2008, <http://www.atmos-chem-phys.net/8/1139/2008/>.

15 Schauer, J. J. and Cass, G. R.: Source apportionment of wintertime gas-phase and particle-phase air pollutants using organic compounds as tracers, *Environ. Sci. Technol.*, 34(9), 1821–1832, 2000.

Schauer, J. J., Kleeman, M. J., Cass, G. R., and Simoneit, B. R. T.: Measurement of emissions from air pollution sources – 3: C-1-C-29 organic compounds from fireplace combustion of wood, *Environ. Sci. Technol.*, 35(9), 1716–1728, 2001.

20 Seinfeld, J. H., Pandis, S. N.: *Atmospheric Chemistry and Physics – From Air Pollution to Climate Change*, John Wiley and Sons, New York, USA, 1998.

Shrivastava, M. K., Lane, T. E., Donahue, N. M., Pandis, S. N., and Robinson, A. L.: Effects of Gas-Particle Partitioning and Aging of Primary Emissions on Urban and Regional Organic Aerosol Concentrations, *J. Geophys. Res.*, in press, 2008.

25 Shrivastava, M. K., Lipsky, E. M., Stanier, C. O., and Robinson, A. L.: Modeling semivolatile organic aerosol mass emissions from combustion systems, *Environ. Sci. Technol.*, 40(8), 2671–2677, 2006.

Stanier, C. O., Pathak, R. K., and Pandis, S.: Measurements of the Volatility of Aerosols from alpha-Pinene Ozonolysis, *Environ. Sci. Technol.*, 41(8), 2756–2763, 2007.

30 Strader, R., Lurmann, F., and Pandis, S. N.: Evaluation of secondary organic aerosol formation in winter, *Atmos. Environ.*, 33(29), 4849–4863, 1999.

Subramanian, R., Khlystov, A. Y., Cabada, J. C., and Robinson, A. L.: Positive and negative

**Laboratory studies of
the atmospheric
aging of wood smoke**

A. P. Grieshop et al.

Title Page

Abstract

Introduction

Conclusions

References

Tables

Figures

◀

▶

◀

▶

Back

Close

Full Screen / Esc

Printer-friendly Version

Interactive Discussion



artifacts in particulate organic carbon measurements with denuded and undenuded sampler configurations, *Aerosol. Sci. Technol.*, 38, 27–48, 2004.

Szidat, S., Jenk, T. M., Synal, H. A., Kalberer, M., Wacker, L., Hajdas, I., Kasper-Giebl, A., and Baltensperger, U.: Contributions of fossil fuel, biomass-burning, and biogenic emissions to carbonaceous aerosols in Zurich as traced by C-14, *J. Geophys. Res.-Atmos.*, 111(D7), D07206, doi:10.1029/2005JD006590, 2006.

Tanner, R., Parkhurst, W., and McNichol, A.: Fossil Sources of Ambient Aerosol Carbon Based on 14C Measurements, *Aerosol. Sci. Technol.*, 38(1 Supplement 1), 133–139, 2004.

Trentmann, J., Andreae, M. O., and Graf, H. F.: Chemical processes in a young biomass-burning plume, *J. Geophys. Res.-Atmos.*, 108(D22), 4705, doi:10.1029/2003JD003732, 2003.

Trentmann, J., Yokelson, R. J., Hobbs, P. V., Winterrath, T., Christian, T. J., Andreae, M. O., and Mason, S. A.: An analysis of the chemical processes in the smoke plume from a savanna fire, *J. Geophys. Res.-Atmos.*, 110(D12), D12301, doi:10.1029/2004JD005628, 2005.

Turpin, B. J. and Lim, H. J.: Species contributions to PM_{2.5} mass concentrations: revisiting common assumptions for estimating organic mass, *Aerosol. Sci. Technol.*, 35(1), 602–610, 2001.

Turpin, B. J., Saxena, P., and Andrews, E.: Measuring and simulating particulate organics in the atmosphere: problems and prospects, *Atmos. Environ.*, 34(18), 2983–3013, 2000.

Watson, J. G.: Visibility: Science and regulation, *J. Air Waste Manage.*, 52(6), 628–713, 2002.

Weitkamp, E. A., Sage, A. M., Pierce, J. R., Donahue, N. M., and Robinson, A. L.: Organic aerosol formation from photochemical oxidation of diesel exhaust in a smog chamber, *Environ. Sci. Technol.*, 41(20), 6969–6975, 2007.

Wotawa, G., and Trainer, M.: The influence of Canadian forest fires on pollutant concentrations in the United States, *Science*, 288(5464), 324–328, 2000.

Zheng, M., Ke, L., Edgerton, E., Schauer, J., Dong, M., and Russell, A.: Spatial distribution of carbonaceous aerosol in the southeastern United States using molecular markers and carbon isotope data, *J. Geophys. Res.*, 111(D10), D10S06, doi:10.1029/2005JD006777, 2006.

**Laboratory studies of
the atmospheric
aging of wood smoke**

A. P. Grieshop et al.

Title Page

Abstract

Introduction

Conclusions

References

Tables

Figures

◀

▶

◀

▶

Back

Close

Full Screen / Esc

Printer-friendly Version

Interactive Discussion



Laboratory studies of the atmospheric aging of wood smoke

A. P. Grieshop et al.

Table 1. Summary of experimental conditions of fresh emissions before turning on the UV lights.

Experiment	MCE	POA	OC:EC	NO _x ^a	Injection		ΔBenzene/ ΔCO ^b	ΔToluene/ ΔCO ^b	ΔAcetonitrile/ ΔCO ^{b,c}	
					ΔCO ^b	ΔCO ₂ ^b				
		μg m ⁻³	ratio	ppb	ppm	molar %	ppb ppm ⁻¹	ppb ppm ⁻¹	ppb ppm ⁻¹	
Laurel Oak										
1	smoldering and flaming	0.90	40	1.6	113	19	17	0.8	0.2	0.1
2	flaming w/ embers	0.95	90	1.9	150	13	7	1.3	0.2	0.3
3	smoldering and flaming	0.93	40	1.1	60	6	11	1.1	0.1	0.5
Yellow Pine										
4	flaming w/ embers	0.92	770	2.2	103 (39)	10	14	4.3	1.5	0.6
5	smoldering/dying flame	0.79	50	13	63	37	41	0.1	0.0	0.1
High NO _x (Pine)										
6	flaming w/ embers	0.69	70	13	244 (18)	2	71	3.7	1.1	0.8

- ^a The values in parenthesis for experiments 4 and 6 show the NO_x levels before additional NO was injected into the chamber
- ^b Values show the increase in chamber concentrations with injection of wood smoke
- ^c Uncertainty in acetonitrile concentrations were about a factor of 2 due to problems with the calibration for this compound during these experiments

Title Page

Abstract

Introduction

Conclusions

References

Tables

Figures

◀

▶

◀

▶

Back

Close

Full Screen / Esc

Printer-friendly Version

Interactive Discussion



Table 2. Summary of experimental parameters related to aerosol aging.

Experiment	(OH) molec cm ⁻³	ΔO_3^a ppb	Aging		AMS O:C ^d initial	AMS O:C ^d final	
			BC-OA ER ^b ratio	SOAM ER ^c Ratio			
Laurel Oak							
1	smoldering and flaming	4.2E+06	148	1.9	1.16	0.36	0.56
2	flaming w/ embers	3.6E+06	275	1.8	1.24	0.34	0.55
3	smoldering and flaming	3.6E+06	102	2.1	1.21	0.25	0.42
Yellow Pine							
4	flaming w/ embers	3.1E+06	220	2.6	1.08	0.13	0.38
5	smoldering/dying flame	3.9E+06	196	2.7	1.25	0.2	0.5
High NO _x (Pine)							
6	flaming w/ embers ^e	2.9E+06	43	1.2	1.15	0.22	0.4

^a ΔO_3 is the increase in chamber O₃ mixing ratio during photo-oxidation

^b BC-OA ER is the end-of-experiment OA ER determined using BC-scaling (Eq. 1)

^c SOAM ER is the predicted SOA formation based on measured VOC precursor decay modeled in SOAM II

^d AMS O:C ratio is determined using the fractional contribution at *m/z* 44 to the AMS organic spectrum and the relation from Aiken et al. (2008)

^e High-NO_x yields from Ng et al. (2007) were used to model SOA formation from aromatics in this experiment

Laboratory studies of the atmospheric aging of wood smoke

A. P. Grieshop et al.

Title Page

Abstract

Introduction

Conclusions

References

Tables

Figures

◀

▶

◀

▶

Back

Close

Full Screen / Esc

Printer-friendly Version

Interactive Discussion



Laboratory studies of the atmospheric aging of wood smoke

A. P. Grieshop et al.

Title Page

Abstract

Introduction

Conclusions

References

Tables

Figures

◀

▶

◀

▶

Back

Close

Full Screen / Esc

Printer-friendly Version

Interactive Discussion



Table 3. Parameters used in basis-set and thermodynamic models.

C^* $\mu\text{g m}^{-3}$	ΔH_{vap} kJ mol^{-1}	Molecular Weight g mol^{-1}	POA volatility distributions ^a	
			Filter only	Filter+IVOC
0.01	77	524	0.03	0.03
0.1	73	479	0.06	0.06
1	69	434	0.09	0.09
10	65	389	0.14	0.14
100	61	344	0.18	0.18
1000	57	299	0.3	0.3
10000	54	254	0.2	0.4
100000	50	208	0	0.5
1000000	46	163	0	0.8

		Robinson et al. (2007)	Modified
k_{OH}	$\text{cm}^3 \text{ molec}^{-1} \text{ s}^{-1}$	4.0×10^{-11}	2.0×10^{-11}
Oxygen	Mass/generation	1.075	1.4
Volatility shift	Bins/generation	1 bin	2 bins

^a Relative mass emissions in each volatility bin

Laboratory studies of
the atmospheric
aging of wood smoke

A. P. Grieshop et al.

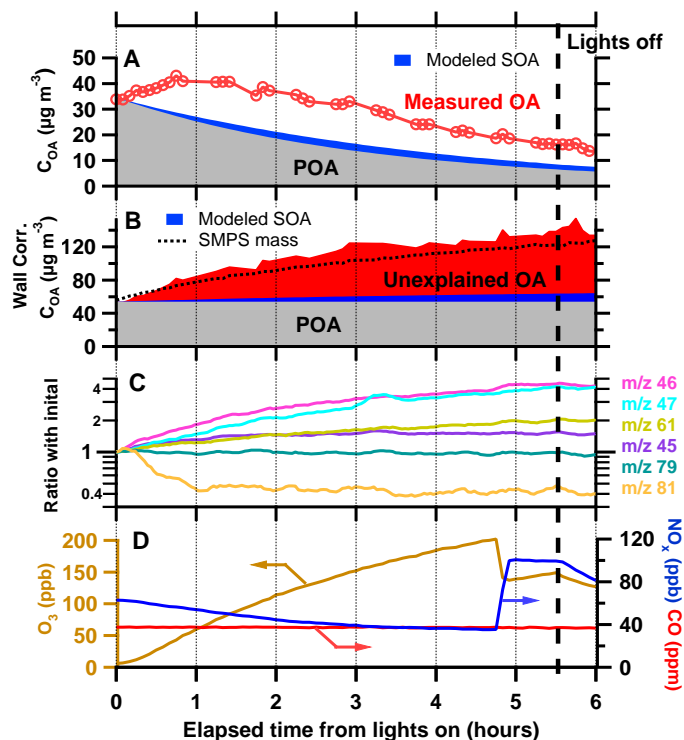


Fig. 1. Time series plots from aging experiment 5 conducted with emissions from smoldering Yellow Pine. **(A)** Measured OA, estimated POA based on BC data, and predicted traditional SOA. **(B)** Wall-loss-corrected OA concentrations of primary, predicted and traditional SOA and total OA based on the BC data (red). The dashed line in (B) is the SMPS wall-loss-corrected estimate. **(C)** PTR-MS data showing the change in relative signal intensity for select mass fragments. **(D)** CO , O_3 and NO_x levels. The large increase in NO_x at hour 4.8 was due to an injection of additional NO into the chamber, which titrated some O_3 .

Title Page

Abstract

Introduction

Conclusions

References

Tables

Figures

◀

▶

◀

▶

Back

Close

Full Screen / Esc

Printer-friendly Version

Interactive Discussion



Laboratory studies of
the atmospheric
aging of wood smoke

A. P. Grieshop et al.

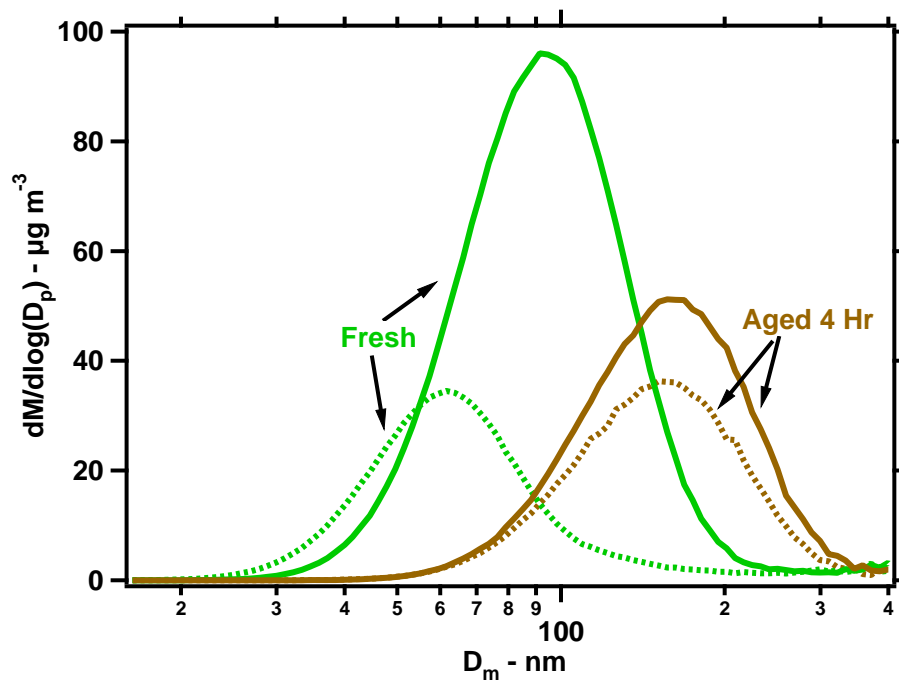


Fig. 2. SMPS mass-weighted particle size distributions measured before the UV lights were turned on (fresh) and after 4 h of aging. Dashed lines show size distributed measured after the aerosol was passed through the TD system at 50°C. Calculations based on a particle density of 1 g cm^{-3} .

[Title Page](#)[Abstract](#)[Introduction](#)[Conclusions](#)[References](#)[Tables](#)[Figures](#)[◀](#)[▶](#)[◀](#)[▶](#)[Back](#)[Close](#)[Full Screen / Esc](#)[Printer-friendly Version](#)[Interactive Discussion](#)

Laboratory studies of
the atmospheric
aging of wood smoke

A. P. Grieshop et al.

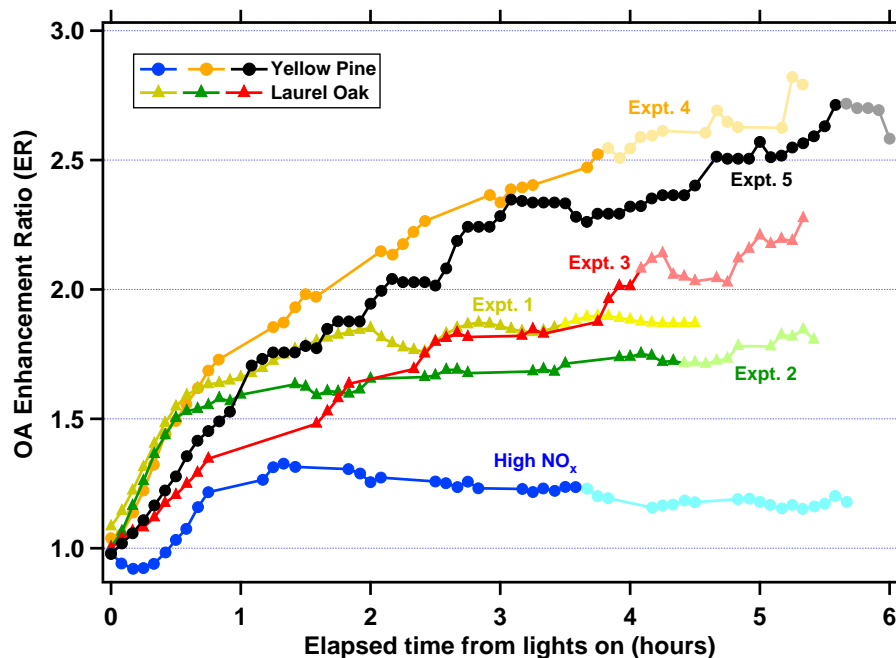


Fig. 3. Compilation of OA ER calculated using AMS and BC data (Eq. 1). The traces are shown in a lighter color after lights-off. Experimental conditions are listed in Tables 1 and 2.

[Title Page](#)[Abstract](#)[Introduction](#)[Conclusions](#)[References](#)[Tables](#)[Figures](#)[◀](#)[▶](#)[◀](#)[▶](#)[Back](#)[Close](#)[Full Screen / Esc](#)[Printer-friendly Version](#)[Interactive Discussion](#)

Laboratory studies of
the atmospheric
aging of wood smoke

A. P. Grieshop et al.

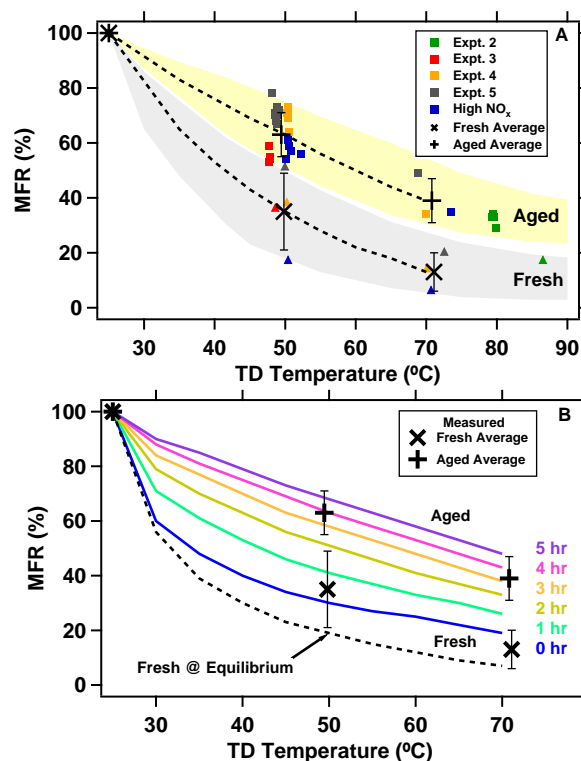


Fig. 4. Thermograms of OA mass fraction remaining (MFR) for fresh and aged aerosols. **(A)** Measured data for five experiments. Data points for fresh OA are shown with triangles and aged OA with squares. The dashed lines in (A) indicate average fresh and aged thermograms. The colored fans in (A) illustrate the inter-experiment variability in the thermal denuder data. **(B)** Comparison of average measured OA MFR values with predicted values based on modified model as discussed in the text. The TD model uses an uptake coefficient of 0.05. The dashed line in (B) indicates TD model predictions assuming that the aerosol has reached equilibrium.

[Title Page](#)[Abstract](#)[Introduction](#)[Conclusions](#)[References](#)[Tables](#)[Figures](#)[◀](#)[▶](#)[◀](#)[▶](#)[Back](#)[Close](#)[Full Screen / Esc](#)[Printer-friendly Version](#)[Interactive Discussion](#)

Laboratory studies of
the atmospheric
aging of wood smoke

A. P. Grieshop et al.

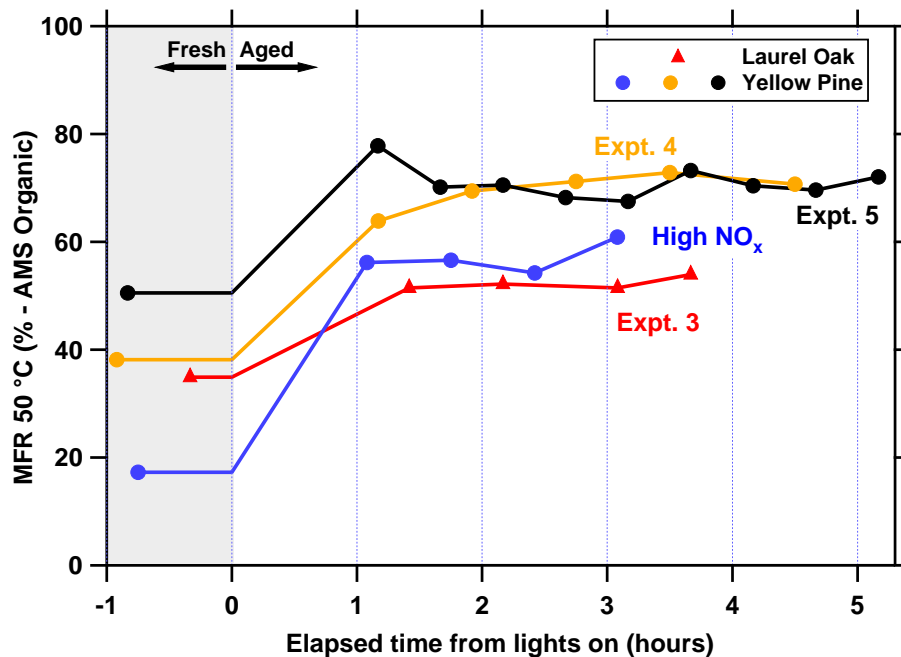


Fig. 5. Time series of OA MFR measured at 50°C for four wood smoke aging experiments.

[Title Page](#)[Abstract](#)[Introduction](#)[Conclusions](#)[References](#)[Tables](#)[Figures](#)[◀](#)[▶](#)[◀](#)[▶](#)[Back](#)[Close](#)[Full Screen / Esc](#)[Printer-friendly Version](#)[Interactive Discussion](#)

Laboratory studies of
the atmospheric
aging of wood smoke

A. P. Grieshop et al.

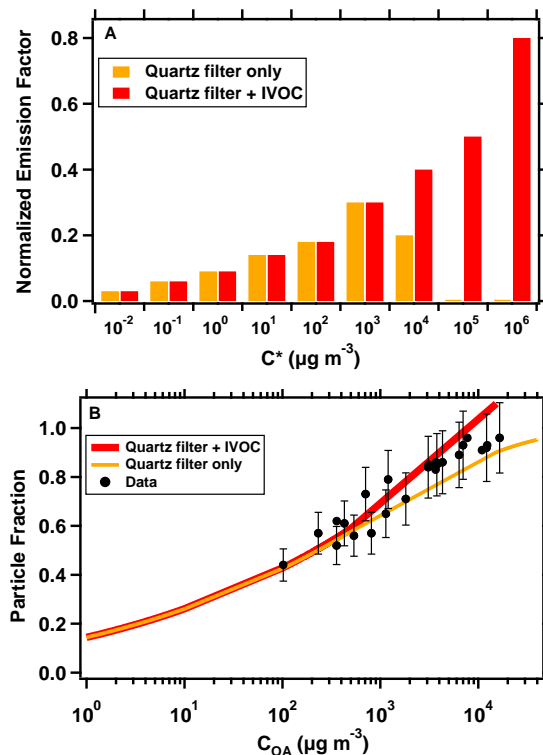


Fig. 6. (A) Volatility distributions proposed by Robinson et al. (2007) for POA. (B) Measured gas-particle partitioning data for wood smoke expressed as the fraction of the semivolatile organics found in the particle phase. The curves in (B) show predicted partitioning based on volatility distributions shown in (A). Measured partitioning data is from wood smoke dilution experiments (Lipsky and Robinson, 2006; Shrivastava et al., 2006).

[Title Page](#)[Abstract](#)[Introduction](#)[Conclusions](#)[References](#)[Tables](#)[Figures](#)[◀](#)[▶](#)[◀](#)[▶](#)[Back](#)[Close](#)[Full Screen / Esc](#)[Printer-friendly Version](#)[Interactive Discussion](#)

Laboratory studies of
the atmospheric
aging of wood smoke

A. P. Grieshop et al.

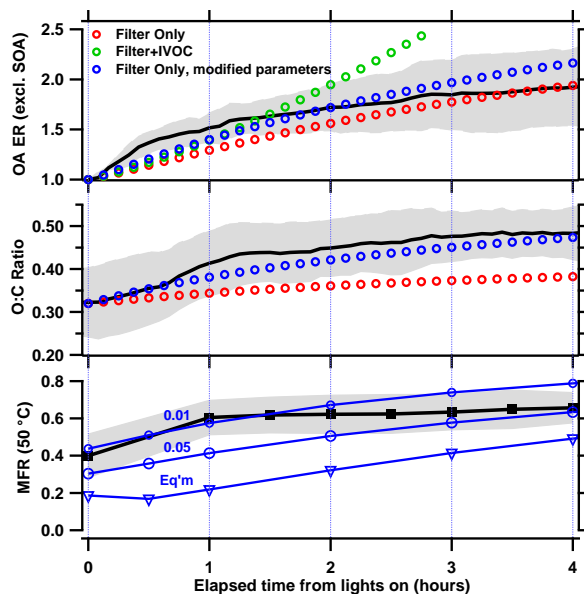


Fig. 7. Time series comparing campaign-average measured and predicted OA: **(A)** Enhancement ratio corrected for traditional SOA; **(B)** OA O:C ratio; **(C)** OA MFR at 50°C. Black lines indicate average data with grey regions showing \pm one standard deviation. The colors of the lines and symbols are used consistently in all three panels; they symbols indicate model predictions using the different sets of parameters listed in Table 3. Numbers in (C) indicate uptake coefficient.

[Title Page](#)[Abstract](#)[Introduction](#)[Conclusions](#)[References](#)[Tables](#)[Figures](#)[◀](#)[▶](#)[◀](#)[▶](#)[Back](#)[Close](#)[Full Screen / Esc](#)[Printer-friendly Version](#)[Interactive Discussion](#)